Effective Segmentation for Dental X-Ray Images Using Texture-Based Fuzzy Inference System

Y.H. Lai[1] and P.L. Lin[2,*]

[1] Department of Computer Science and Engineering
National Chung Hsing University, Taichung 40227, Taiwan
yanhao.lai@gmail.com
[2] Department of Computer Science and Information Engineering
Providence University, Shalu, Taichung 43301, Taiwan
lan@pu.edu.tw

Abstract. In teeth-related radiograph research, the information of teeth shape is the most critical factor for achieving highly automated diagnosis. Therefore, accurate segmentation is an essential but difficult task due to low contrast and uneven exposure of the dental X-ray image. In this paper, we propose a novel scheme to automatically segment teeth by using texture characteristics instead of primitive intensity or edge used in previous researches. At first, image enhancement based on homogeneity measurement is applied to accentuate the texture of gums while smoothing the teeth so that a coarse clustering result can be obtained. Then, fuzzy inference is applied to speculate degrees of pixel belonging to either part. Finally, region growing based on inferences is performed to obtain the complete shape of teeth. The experimental results show that our proposed method indeed outperforms the methods using direct intensity or edge in segmenting complete teeth from X-ray dental images.

Keywords: Dental X-ray image, Adaptive Local Contrast Stretching, Image Clustering, Fuzzy Inference System, Region Growing.

1 Introduction

In dental clinic practices, radiographs (X-ray images) can assist dentists to diagnose many dental anomalies, as most anomalies are hidden under the surface and can not be seen during a visual examination [8]. As the usage of digital dental X-ray images keep growing, computer aided analyses become highly desirable for improving the accuracy and efficiency of treatment planning and individual identification from the enormous database. However, automatic dental X-ray analysis is still a challenging issue up-to-date.

Jain and Chen [5] proposed a semi-automatic contour extraction method for tooth segmentation by using integral projection and Bayes rule, in which the integral projection is semi-automatically applied for tooth isolation since an initial valley gap point is required. Zhou and Abdel-Mottaleb [18] presented a segmentation method that consists of three steps: image enhancement, region of interest localization, and

* Corresponding author.

J. Blanc-Talon et al. (Eds.): ACIVS 2008, LNCS 5259, pp. 936–947, 2008.

tooth segmentation by using morphological operations and Snake method. Nomir and Abdel-Mottaleb [12] developed a fully automated approach based on iterative thresholding and adaptive thresholding for dental X-ray image segmentation. Keshtkar and Gueaieb [7] introduced a swarm-intelligence based and a cellular-automata model approach for segmenting dental radiographs. Said et al. [14] offered a mathematical morphology approach to the problem of teeth segmentation, which used a series of morphology filtering operations to improve the segmentation, and then analyzed the connected components to obtain the desired region of interests (ROIs). Li et al. [8] proposed a semi-automatic lesion detection framework by using two coupled level set functions in which initial contour are derived from a trained support vector machine to detect areas of lesions from dental X-ray images.

Figure 1(a) shows a general dental X-ray image. In teeth segmentation, the two major problems causing incorrect result are: (1) Lack of clear edges between teeth and gums due to substantial noise and complicated structures. Figures 1(b) and 1(c) show the results of using two different edge-based methods. (2) Poor image quality due to low contrast and uneven exposure that makes both intensities of gums and teeth very close. Figures 1(d) and (e) show the results of Said et al. [14] and Nomir [12] using intensity only. As we can see that both results are either insufficient or confused for acquiring complete teeth shape.

To overcome the aforementioned problems, instead of directly using grayscale intensity for segmentation, we propose a novel method to automatically segmenting teeth by using texture. At first, an image enhancement based on the homogeneity measurement is applied to differentiate textures between gums and teeth for clustering. Then, fuzzy inference is applied to speculate degrees of pixel belonging to either part according to a set of membership functions associated with textures and clustering result. Finally, region growing is performed to obtain the complete shape of teeth.

The remainder of the paper is organized as follows. Section 2 introduces our proposed image enhancement method for improving texture discrimination between gums and teeth. Section 3 describes our teeth clustering method based on texture characteristics. A fuzzy inference system for computing degree of "belonging to" of pixels is shown in Section 4. Then, a region growing algorithm for segmenting complete teeth is presented in Section 5. Experimental results that demonstrate the

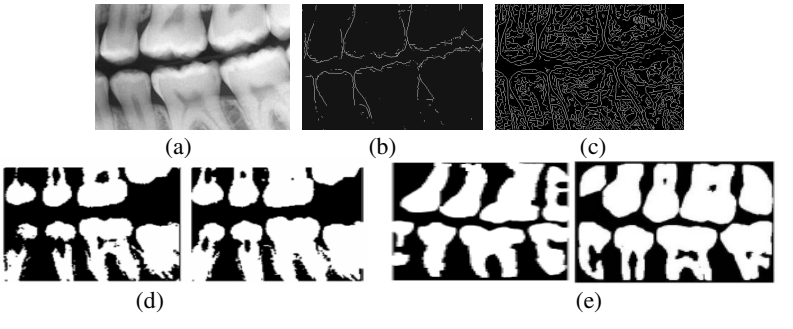

Fig. 1. (a) General dental X-ray image. Edge detection results by (b) Sobel operator (c) Canny algorithm. Segmentation results by (d) Said et al. [14] (e) Nomir and Abdel-Mottaleb [12].

effectiveness of our proposed method are shown in Section 6. Finally, the conclusions are given in Section 7.

2 Dental X-Ray Image Enhancement

Dental X-ray images always suffer from problems like noise, low contrast, and uneven exposure. In order to successfully separate teeth apart from background and gums, we firstly apply adaptive local contrast stretching to increase texture differentiation between teeth and gums. We then apply adaptive morphological enhancement to further accentuate the cobweb-like texture within gums.

2.1 Adaptive Local Contrast Stretching

Global enhancement, such as histogram equalization and global Power-law transformation is neither efficient nor effective for uneven exposure dental X-ray images, as the results of applying these two methods are either over- or under-enhanced. On the other hand, when contrast is stretched based on the local discrepancy, the uneven exposure problem can be greatly reduced [11]. In this proposed method, we use a local homogeneity measurement as the basis for adaptive local contrast stretching to enhance dental X-ray images.

2.1.1 Homogeneity Measurement

Homogeneity is a mathematic statistic measurement that relates to the local information and reflects the degree of uniformity in a region of interest [1]. Our homogeneity measurement is based on three local discrepancy measurements: Local range value, Standard deviation, and Gamma 4.

- *Local Range Value*

Local range measures the difference between the maximum and the minimum value of the neighborhood pixels within a window $w(x, y)$ centered at (*x*,*y*), and is defined as:

$$d(x, y) = max\{g(x+p, y+q)\} - min\{g(x+p, y+q)\}. \tag{1}$$

where $p = -\lfloor w/2 \rfloor \sim \lfloor w/2 \rfloor, q = -\lfloor w/2 \rfloor \sim \lfloor w/2 \rfloor.$

- *Local Standard Deviation*

Standard deviation describes the dispersion within a local region, and can be computed as:

$$v(x, y) = \sqrt{\frac{1}{w^2} \sum_{p=-\lfloor w/2 \rfloor}^{\lfloor w/2 \rfloor} \sum_{q=-\lfloor w/2 \rfloor}^{\lfloor w/2 \rfloor} [g(x+p, y+q) - \mu(x, y)]^2}. \tag{2}$$

where $$\mu(x, y) = \frac{1}{w^2} \sum_{p=-\lfloor w/2 \rfloor}^{\lfloor w/2 \rfloor} \sum_{q=-\lfloor w/2 \rfloor}^{\lfloor w/2 \rfloor} g(x+p, y+q). \tag{3}$$

- *Gamma 4 (γ_4)*

γ_4 defines the impulsiveness of the distribution, which can be computed through

$$\gamma_4(x,y)=\frac{\sum_{p=-\lfloor w/2\rfloor}^{\lfloor w/2\rfloor}\sum_{q=-\lfloor w/2\rfloor}^{\lfloor w/2\rfloor}\left[g(x+p,y+q)-\mu(x,y)\right]^4}{w^2-1}. \tag{4}$$

- *Our Homogeneity Measurement*

We define Homogeneity Measurement as a combination of the complement of the above three features as

$$H(x,y)=\left(1-D(x,y)\right)\times\left(1-V(x,y)\right)\times\left(1-R_4(x,y)\right) \tag{5}$$

where $D(x, y)$, $V(x,y)$, $R_4(x,y)$ are the normalized value of $d(x,y)$, $v(x,y)$, and $\gamma_4(x,y)$, respectively, i.e.,

$$D(x,y)=\frac{d(x,y)}{max\{d(x,y)\}}, V(x,y)=\frac{v(x,y)}{max\{v(x,y)\}}, R_4(x,y)=\frac{\gamma_4(x,y)}{max\{\gamma_4(x,y)\}}. \tag{6}$$

Note that if the values of $D(x,y)$, $V(x,y)$, and $R_4(x,y)$ in the region are all 0, the region is then considered as perfectly uniform, and the more uniform a region is, the larger the homogeneity measurement of the pixel will be.

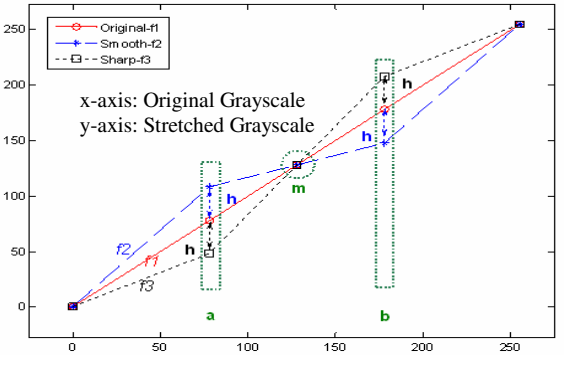

Fig. 2. Three adaptive local contrast stretching functions

2.1.2 Adaptive Contrast Stretching

In dental X-ray images, pixels within gums appeared not as smooth as those in teeth part, i.e., they have higher non-homogeneity than those in teeth. Thus, for further smoothing teeth and sharpening gums in a dental X-ray image, we propose an adaptive piecewise linear stretching function, as shown in Fig. 2, based on local homogeneity measurement. The stretching function is constructed as follows.

(1) Calculate the degree of non-homogeneity $NH(x,y)$ for each pixel (x,y) by:

$$NH(x,y)=1-\frac{H(x,y)}{max\{H(x,y)\}}. \tag{7}$$

(2) Compute the mean non-homogeneity gray value $\delta(x, y)$ for window $w(x, y)$ centered at pixel (x,y). This represents the control point "m" of the stretching function.

$$\delta(x, y) = \frac{\sum_{p=-\lfloor w/2 \rfloor}^{\lfloor w/2 \rfloor} \sum_{q=-\lfloor w/2 \rfloor}^{\lfloor w/2 \rfloor} \left[g(x+p, y+q) \times NH(x+p, y+q) \right]}{\sum_{p=-\lfloor w/2 \rfloor}^{\lfloor w/2 \rfloor} \sum_{q=-\lfloor w/2 \rfloor}^{\lfloor w/2 \rfloor} NH(x+p, y+q)}. \tag{8}$$

(3) Determine the other control points "a", "b", and slope "h" using the control point "m", local homogeneity measurement NH, and standard deviation v as follows.

$$h = v(x, y) * NH(x, y) * C, \quad where \quad NH(x, y) \in [-1, 1]. \tag{9}$$

$$\begin{cases} a\_x = \delta(x, y) - v(x, y) \\ b\_x = \delta(x, y) + v(x, y) \end{cases}, \begin{cases} a\_y = a\_x - h \\ b\_y = b\_x + h \end{cases} \tag{10}$$

where a_x, a_y, b_x, and b_y denote the coordinate of control points "a" and "b", respectively.

Note that the range of $NH(x,y)$ in (9) is extended to [-1,1] from [0, 1]. The region is smooth when the value is negative, and the larger the absolute value, the more uniform the region (i.e. teeth part). On the other hand, positive value means lots of textures existed in the region (i.e. gums). The parameter C is a magnification constant. Thus, a smooth function and a sharp function are constructed for teeth and gums, respectively.

(4) Map every pixel in image IM to a new value $IM_c(x, y)$ one-by-one according to the adaptive stretching function as follows:

$$IM_c(x, y) = \begin{cases} (a\_y / a\_x) * IM(x, y), & \text{if} \quad IM(x, y) \le a\_x \\ (b\_y - a\_y) / (b\_x - a\_x) * (IM(x, y) - a\_x) + a\_y, & \text{if} \quad a\_x < IM(x, y) < b\_x \\ (255 - b\_y) / (255 - b\_x) * (IM(x, y) - b\_x) + b\_y, & \text{if} \quad IM(x, y) \ge b\_x \end{cases} \tag{11}$$

2.2 Adaptive Morphological Enhancement

After applying the adaptive local contrast stretching, the teeth become smoother, and the gums become more textured. To further increase their texture discrepancy, cobweb-like texture in the gums can be used as another discrimination characteristic. For accentuating the cobweb-like texture, which has small bright and dark spots, without influencing the background, we use the combination of morphological top-hat and bottom-hat transformations [10] onto the enhanced image IM_c to further emphasize the texture in the gums by:

$$IM_E(x, y) = IM_c(x, y) + (T(x, y) - B(x, y)) * NH(x, y). \tag{12}$$

where
$$T(x,y) = IM(x,y) - (IM(x,y) \circ S).$$
$$B(x,y) = (IM(x,y) \bullet S) - IM(x,y).$$

and S is a disk structure element with radius 3. Non-homogeinity NH is used to avoid the affect of noise. The operators $\circ$ and $\bullet$ represent morphological opening and closing used in Top-hat transformation T and Bottom-hat transformation B, respectively.

3 Image Clustering

According to the higher discrimination of texture in the enhanced image, we use two characteristics of texture (Entropy and Edge-value) and intensity as feature vectors for classifying dental X-ray into three clusters: background, teeth, and gums.

- *Entropy*

Entropy is a measurement with regard to the amount of information and degree of randomness in the region [4] [15]. It can be calculated as

$$r(x,y) = -\sum_{i=1}^{L} p(z_i)\log_2 p(z_i). \tag{13}$$

where z is a random variable, $p(z_i)$ represents the probability of ith grayscale value, i=1,2,…,L, L is the total number of distinct grayscale values.

- *Edge-value*

Edge-value stands for the number of abrupt changes in a region, and can be defined as the number of edges in the region.

$$e(x,y) = \sum_{p=-\lfloor w/2 \rfloor}^{\lfloor w/2 \rfloor} \sum_{q=-\lfloor w/2 \rfloor}^{\lfloor w/2 \rfloor} b(x,y) \tag{14}$$

where $b(x,y) = \begin{cases} 1, & \nabla f(x,y) \geq T1 \\ 0, & \nabla f(x,y) < T1 \end{cases}$, $\nabla f(x,y) = \sqrt{\left(\frac{\partial g(x,y)}{\partial x}\right)^2 + \left(\frac{\partial g(x,y)}{\partial y}\right)^2}$

and $\nabla f(x,y)$ means the magnitude of gradient, $b(x,y)$ is a binary image, $g(x,y)$ is intensity of X-ray image, and $T1$ is the threshold value.

- *K-means Clustering*

K-means [6] is a prototype-based clustering algorithm that attempts to cluster pixels into a user-specified number of clusters K according to extracted feature vectors. In our application, the three normalized feature vectors: entropy $R(x,y)$, edge-value $E(x,y)$, and intensity $G(x,y)$ are used as feature vectors of clustering:

$$R(x,y) = \frac{r(x,y)}{max\{r(x,y)\}}, E(x,y) = \frac{e(x,y)}{max\{e(x,y)\}}, G(x,y) = \frac{g(x,y)}{max\{g(x,y)\}} \tag{15}$$

At first, $K(=3)$ initial centroids are chosen randomly from the normalized feature vectors for representing background, teeth, and gums in a dental X-ray image. Each point is then assigned to the closest centroid to form a cluster. When all of points are finished, the centroid of each cluster is recomputed. Repeating the pixel assignment and centroid updating until no point can change the clusters. Figure 4(f) shows the result of *K*-means clustering, in which teeth can be roughly distinguished from background and gums. However, to obtain complete shape, the teeth part needs to be further expanded for better close to the real contour of teeth.

4 Fuzzy Inference System Construction

Fuzzy inference system (FIS) [9][17], which mainly consists of a fuzzification interface, rule base, and a defuzification interface, has been well known for providing a convenient handling of uncertain values. To obtain a near-true teeth shape, we construct a fuzzy inference system based on the texture vectors and the clustering result to produce a membership for each pixel.

4.1 Fuzzification Interface

Nine linguistic variables used in rule base, six for inputs and three for outputs. The input variables include "*Entropy*", "*Edge-value*", "*Intensity*", "*Background-distance (BD)*", "*Tooth-distance (TD)*", and "*Gum-distance (GD)*", and the output variables contain "*Background*", "*Tooth*", and "*Gum*". All of these nine variables have linguistic terms: "*Low*", "*Medium*", and "*High*". For each linguistic term, we define a membership function to compute the score of membership about an input linguistic variable.

- *Entropy, Edge-value, Intensity variables*

Piecewise linear functions are adopted as the membership functions for these three variables. The fuzzy set "*Low*" in texture vectors can be interpreted as the membership of "low value group", while the fuzzy set "*Medium*" and "*High*" denote the membership of "medium value group" and "high value group", respectively. The equation (16) is an example of piecewise linear functions associated with "*Medium*".

$$\mu_{medium}(x) = \begin{cases} 0, & x \le PL \\ \dfrac{x - PL}{PM - PL}, & PL < x \le PM \\ \dfrac{PH - x}{PH - PM}, & PM < x \le PH \\ 0, & x > PH \end{cases} \tag{16}$$

where x is the linguistic variable, *PL*, *PM*, and *PH* are the center of background, teeth, and gums cluster in clustering result, respectively.

- *BD, TD, GD, Background, Tooth and Gum*

The adopted membership functions for *BD*, *TD*, *GD*, *Background, Tooth* and *Gum* are Gaussian functions with means 0, 0.5, and 1 associated with "*Low*", "*Medium*", and "*High*", respectively. *BD*, *TD*, and *GD* represents the distance computed from coordinate of each pixel to *PL*, *PM*, and *PH*, respectively. The output variables, *Background*, *Tooth*, and *Gum* show the membership degree of pixel x belonging to each fuzzy set.

4.2 Rule Base

Fuzzy rules can be used to compute the rule strength and obtain the fuzzy output distribution. We define two sets of fuzzy rules: one for separating the teeth from background, the other for differentiating between teeth and gums. For easier presentation, we denote "*L*", "*M*", and "*H*" for membership function "*Low*", "*Medium*", and "*High*", respectively, and "*&*", "|" for fuzzy logic "*AND*" and "*OR*", respectively.

(1) Fuzzy rules for distinguishing teeth and background
- *(Intensity==“L”) | (BD==“L”) => (Tooth=“L”) & (Background=“H”)*
- *(Entropy~=“L”) | (Edge-Value~=“L”) | (Intensity~=“L”) | (BD~=“L”) | (TD==“L”) | (GD==“L”) | => (Tooth=“H”) & (Background=“L”)*
- *(Edge-value==“M”) & (Intensity==“L”) & (BD~=“H”) => (Background=“M”)*
- *(Entropy==“M”) & (TD~=“H”) & (GD~=“H”) => (Tooth=“M”)*
- *(Intensity==“M”) & (BD~=“L”) & (TD~=“H”) & (GD~=“H”) => (Tooth=“H”) & (Background=“L”)*

(2) Fuzzy rules for distinguishing teeth and gums
- *(Entropy~=“H”) | (Edge-Value~=“H”) | (BD~=“H”) | (TD~=“H”) | (GD~=“L”) => (Tooth=“H”) & (Gums=“L”)*
- *(Entropy==“H”) | (Edge-Value==“H”) | (GD==“L”) => (Tooth=“L”) & (Gums=“H”)*
- *(Entropy==“M”) & (Edge-Value==“M”) & (Intensity==“H”) => (Tooth=“H”) & (Gums=“L”)*
- *(Edge-Value~=“H”) & (Intensity==“H”) & (TD==“M”) & (GD==“M”) => (Tooth=“M”)*
- *(Entropy==“H”) & (Intensity==”M”) & (TD==“M”) & (GD==”M”) => (Gums=”M”)*

4.3 Defuzzification Interface

After fuzzifying the inputs using the membership function and combining the fuzzified inputs according to a sequence of rules, an output distribution can be obtained by combining the consequences. A defuzzifiction process is then applied to convert the output distribution into a single crisp output. In this inference system, we take the output distribution and find its centriod as the single output.

5 Tooth Segmentation

Region growing is a method that collects pixels into a larger region [3][13][16]. It takes a set of seeds as input and grows them up iteratively by comparing all unallocated neighboring pixels to the seeds until no more pixels satisfy the criteria.

In dental X-ray images, teeth have two different kinds of neighboring pixels: background at the top portion (crown) and gums at the bottom portion (root). Thus, we use two different procedures for growing seeds to their neighboring pixels, depending on their positioning in crown or root, respectively. The two procedures are:

(1) If the seed points belong to the crowns:
- Compute the degrees of belonging to tooth and background using the first set of fuzzy rules mentioned in section 4.2.

- Grow if the degree of pixel belonging to tooth > pixel belonging to background by a threshold *T2*.
- Otherwise, grow when the absolute difference of intensities between pixel and seed is less than a threshold *T3*

(2) If the seed points belong to the roots:
- Compute the degrees of belonging to tooth and gum using the second set of fuzzy rules mentioned in section 4.2
- Grow if the degree of pixel belonging to tooth > pixel belonging to gum by a threshold *T2*.
- Otherwise, grow when the absolute difference of both the average intensity and the standard deviation between pixel and seed are less than a threshold *T3* and *T4*, respectively.

The whole segmentation procedure is as follows:

At first, we find the tips of bones from the clustering result, and connect them to separate a dental X-ray image into two sections: one includes crowns and background, the other includes roots and gums. Then we randomly select seed points within teeth and start region growing iteratively using the above criteria until no points satisfied. A morphological operation is applied into root part to reduce the influence of edge between teeth and gums caused by the texture transformation. Finally, we use equal point sampling to select the candidate points along the boundary of tooth, and use them as control points for a *B-spline* function [2] to obtain smooth shape for teeth.

6 Experimental Results

The parameters used in the experiments are: window size w for homogeneity measurement is 5×5 and for feature vectors extraction in clustering is 11×11, the thresholds $T1$=4, $T2$=0.1, $T3$=3 and $T4$=15.

Figure 3 shows the enhanced result of a dental X-ray image. We can see that: (1) the edges between teeth and gums turn more apparent, (2) the contrast within the gums is sharper, (3) the texture of gums is even more accentuated, and (4) both the dark and bright spots are more emphasized and more obvious as shown in Fig. 3(b).

Figure 4 shows the transformed results of the enhanced image based on entropy and edge-value, and the clustering result. Notice that the discrepancies of textures between teeth and gums in 4(b) and 4(d) are more apparent than those in 4(a) and 4(c). Comparing with the result of clustering based on intensity only that some teeth are confused with gums, as shown in Fig. 4(e), we can clearly see that the teeth can be indeed differentiated from background and gums, as shown in 4(f).

However, observing Fig. 4(f), teeth shape is not yet perfectly enclosed, as some pixels within teeth are not classified into teeth cluster. Thus, we construct a FIS to assess membership degree to each cluster for each pixel. Figures 5(a), (b), and (c) show the membership functions that are generated from the clustering result, and Fig. 5(d) illustrates the defuzzification step according a set of fuzzy rules. Figure 6(a) is a set of eroded teeth region selected from Fig. 4(f), and Fig. 6(b) shows the result after region growing. The final result of teeth segmentation is in Fig. 6(c), where the contour of teeth is generated by using B-spline function. The result demonstrates that our proposed scheme can effectively segment the teeth from a dental X-ray image.

(a) (b) (c) (d)

Fig. 3. An example of dental X-ray image enhancement. (a) An original image. (b) Enhanced result. (c) and (d) A portion of images in (a) and (b), respectively.

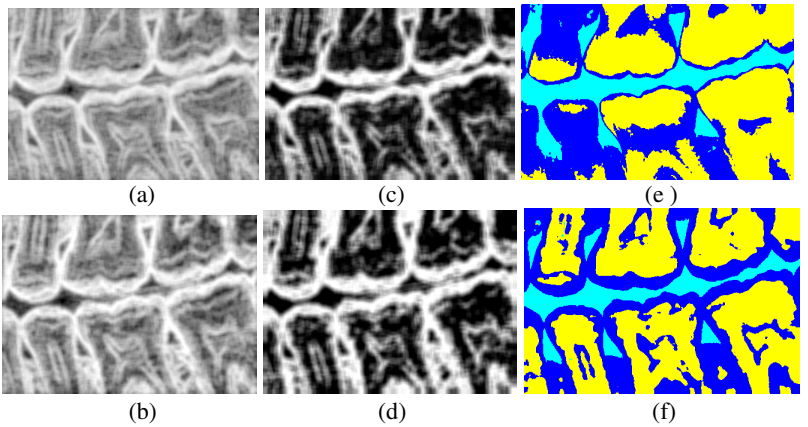

(a) (c) (e)

(b) (d) (f)

Fig. 4. The results of texture transformation: (a), (b) the entropy transformation; (c), (d) the edge-value transformations. (e) The clustering result using intensity only. (f) The clustering result using textures and intensity.

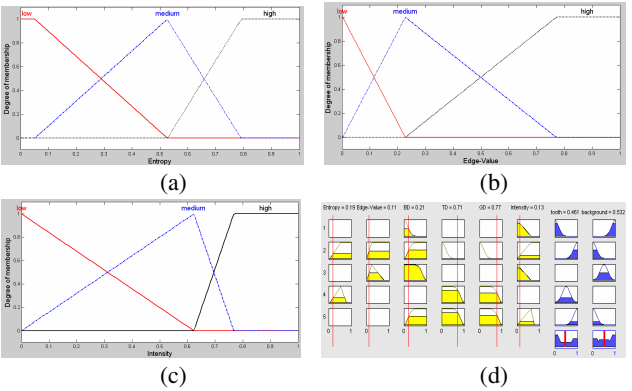

(a) (b)

(c) (d)

Fig. 5. Three membership functions associated with (a) "*Entropy*", (b) "*Edge-value*", and (c) "*Intensity*" variables. (d) An example of defuzzification by a set of fuzzy rules.

(a) (b) (c)

Fig. 6. The result of teeth segmentation. (a) A set of initial seed points. (b) Result of segmentation after region growing. (c) Contour of teeth generated by B-spline function.

7 Conclusions

Dental X-ray images play an important role for achieving individual identification and diagnosis. However, due to variations of shape and intensity as well as low contrast within X-ray images, the segmentation of teeth is still a difficult task. In this paper, we proposed a novel strategy for accurately segmenting teeth from other parts. At first, adaptive local contrast stretching is applied to increase the contrast between teeth and gums. Then, the adaptive morphological top-hat and bottom-hat transformations are applied for accentuating both the dark and bright spots within the gums. Secondly, we used characteristics of texture instead of direct intensity to cluster image roughly to background, teeth, and gums. For more precisely assigning pixel to the teeth part, we used nine linguistic variables, three linguistic terms, and two sets of fuzzy rules to construct a fuzzy inference system to estimate degree of "belonging to" for each pixel. Finally, region growing and B-spline function are used to obtain complete shape of teeth and extract smooth contour of teeth. The experimental results show that our proposed method indeed outperforms the methods using direct intensity or edge in segmenting complete teeth from X-ray dental images.

References

1. Cheng, H.D., Xue, M., Shi, X.J.: Contrast Enhancement Based on a Novel Homogeneity Measurement. Pattern Recognition 36, 2687–2697 (2003)
2. de Boor, C.: B-Spline Basics, Fundamental Developments of Computer-Aided Geometric Modeling, pp. 27–49. Academic Press, New York (1993)
3. Fan, J., Zeng, G., Body, M., Hacid, M.: Seeded Region Growing: An Extensive and Comparative Study. Pattern Recognition Letter 26, 1139–1156 (2005)
4. Gonzalez, Woods: Digital Image Processing, 2 edn. Prentice Hall, Englewood Cliffs (2002)
5. Jain, A.K., Chen, H.: Matching of Dental X-ray Images for Human Identification. Pattern Recognition 37, 1519–1532 (2004)
6. Kanungo, T., Mount, D.M., Netanyahu, N., Piatko, C., Silverman, R., Wu, A.Y.: An Efficient K-means Clustering Algorithm: Analysis and Implementation. IEEE Transaction on Pattern Analysis and Machine Intelligence 24, 881–892 (2002)
7. Keshtkar, F., Gueaieb, W.: Segmentation of Dental Radiographs Using a Swarm Intelligence Approach. In: IEEE Canadian Conference on Electrical and Computer Engineering, pp. 328–331 (2006)

8. Li, S., Fevens, T., Krzyzak, A., Jin, C., Li, S.: Semi-automatic Computer Aided Lesion Detection in Dental X-rays Using Variational Level Set. Pattern Recognition 40, 2861–2873 (2007)
9. Miosso, C.J., Bauchspiess, A.: Fuzzy Inference System Applied to Edge Detection in Digital Images. In: Proceedings of the V Brazilian Conference on Neural Networks, pp. 481–486 (2001)
10. Moragas, A., Garcia-Bonafe, M., de Torres, I., Sans, M.: Textural Analysis of Lymphoid Cells in Serous Effusions. A Mathematical Morphologic Approach. Analytical and Quantitative Cytology and Histology 15, 165–170 (1993)
11. Mukhopadhyay, S., Chanda, B.: A Multiscale Morphological Approach to Local Contrast Enhancement. Signal Processing 80, 685–696 (2000)
12. Nomir, O., Abdel-Mottaleb, M.: A System for Human Identification from X-ray Dental Radiographs. Pattern Recognition 38, 1295–1305 (2005)
13. Pham, D.L., Xu, C., Prince, J.: A Survey of Current Methods in Medical Image Segmentation. Annual Review of Biomedical Engineering 2, 315–337 (2000)
14. Said, E.H., Nassar, D.E.M., Fahmy, G., Ammar, H.H.: Teeth Segmentation in Digitized Dental X-Ray Films Using Mathematical Morphology. IEEE Transactions on Information Forensics and Security 1, 178–189 (2006)
15. Shapiro, L.G., Stockman, G.C.: Computer Vision. Prentice-Hall, Englewood Cliffs (2001)
16. Shih, F.Y., Cheng, S.: Automatic Seeded Region Growing for Color Image Segmentation. Image and Vision Computing 23, 844–886 (2005)
17. Siler, W., Buckley, J.J.: Fuzzy Expert Systems and Fuzzy Reasoning. John Wiley, Chichester (2005)
18. Zhou, J., Abdel-Mottaleb, M.: A Content-based System for Human Identification Based on Bitewing Dental X-ray Images. Pattern Recognition 38, 2132–2142 (2005)